Research Paper

Effect of Silver Nanoparticles with Indium Tin Oxide Thin Layers on Silicon Solar Cells

Gyujin Oh and Eun Kyu Kim*

Department of Physics and Research Institute for Convergence of Basic Sciences, Hanyang University, Seoul 04763, Korea

Abstract AThe effect of localized surface plasmon on silicon substrates was studied using silver nanoparticles. The nanoparticles were formed by self-arrangement through the surface energy using rapid thermal annealing (RTA) technique after the thin nanolayer of silver was deposited by thermal evaporation. By the theoretical calculation based on Mie scattering and dielectric function of air, indium tin oxide (ITO), and silver, the strong peak of scattering cross section of silver nanoparticles was found at 358 nm for air, and 460 nm for ITO, respectively. Accordingly, the strong suppression of reflectance under the condition of induced light of 30° occurred at the specific wavelength which is almost in accordance with peak of scattering cross section. When the external quantum efficiency was measured using silicon solar cells with silver nanoparticles, there was small enhancement peak near the 460 nm wavelength in which the light was resonated between silver nanoparticles and ITO.

Keywords: Ag nanoparticle, Localized surface plasmon resonance, Application to solar cells

I. Introduction

The effect of localized surface plasmon is localized effect of surface plasmon resonance in the tiny metal particles. This resonance effect is determined by various conditions of particles such as size, shape, and dielectric function of particles. Main feature of this effect is that the particles in the specific dielectric environment shows strong peak or scattering cross section in the selective wavelength of light [1-3]. Therefore, there was an amount of attempts to enhance light emitting diodes (LED) based on particular wavelength [4,5]. However, the enhancement of light is the issue not only for the LED, but also for the many kinds of photonic devices including solar cells [6-8]. In the early years of studying on plasmonic effect for solar cells, the research was performed for the thin film solar cells. From the problems like price and flexibility, there have been many studies on the thin film solar cells. The thin film solar cells which are different from the solar cells based on wafer substrates, has active layers with hundreds of nanometers thick. The thickness of layer act as disadvantage fabricating the surface texturing which has several microns for the multiple reflection of light within the textures to make efficient absorption [9]. With the anti-reflection coatings using multi-layers, the plasmon effect was a possible candidate for the anti-flection effect accompanying with enhancement of light absorption.

In this paper, silver nanoparticles with ITO on the silicon substrates was examined. Indium tin oxides (ITO) has been extensively used on various kinds of solar cells regardless of organic and inorganic devices. That is because ITO has good electrical conductivity as well as moderate work function (4.3 eV), and high optical transmittance over 80% [10-12]. Therefore, research on combination of silver nanoparticles and indium tin oxide can become the valuable information for fabricating the solar cell with plasmonic structures. After making the silver nanoparticles under several conditions, theoretical calculations were performed to analyze the reflection properties of Ag nanoparticles on and within ITO thin films (100 nm). Finally, the Ag plasmonic structures were applied to solar cells, and external quantum efficiency (EQE) was evaluated.

II. Experiments and Discussion

To see the light scattering by plasmonic resonance with ITO thin films, the samples are separated with two groups. The first group of samples contains silver nanoparticles on the ITO surface accumulated on silicon substrate (Ag nanoparticles/ITO/Si), and the second group of samples contains silver nanoparticles between ITO and silicon substrates (ITO/Ag nanoparticles/Si). The thickness of ITO for all plasmonic structures was constant value of 100 nm and the ITO thin films were fabricated by radio frequency magnetron sputtering systems. To form Ag nanoparticles, first of all, Ag thin films were deposited by thermal

*Corresponding author
E-mail: ek-kim@hanyang.ac.kr
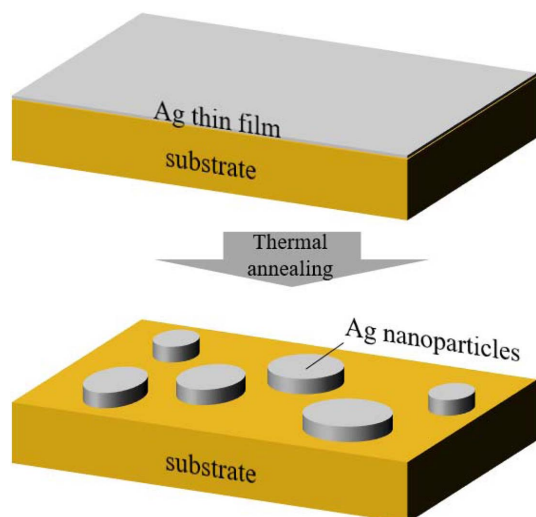
Figure 1. Formation of Ag nanoparticle after rapid thermal annealing process using Ag thin film on a substrate. The substrates which is used in this experiment is indium tin oxide thin layer on silicon substrates or solely the silicon substrate.

Figure 2. Scanning electron microscopy image of Ag thin films, (a) before rapid thermal annealing (Ag 5 nm), (b) after rapid thermal annealing process at 140ºC (Ag 5 nm), and (c) after rapid thermal annealing process at 140ºC (Ag 6 nm).

evaporation and the thickness was 5, 6, 7, 8 nm. Using rapid thermal annealing at 140ºC for 5 minutes, the Ag thin films were thermally treated. After sample preparation, dielectric function and thickness of each films were evaluated by ellipsometry analysis (Ellipso Technology, Elli-SE), and the surface morphology was investigated by scanning electron microscopy (SEM) and atomic force microscopy (AFM, Park systems, XE-100).

Figure 1 shows the formation of Ag nanoparticles after rapid thermal annealing (RTA) process. Ag material on the particular substrates (ITO/Si or Si) using thermal evaporation methods, is deposited as thin films. After RTA process, silver makes self-arrangement in shape of island because of surface energy at the relatively high temperature (here, 140ºC). Through that, Ag nanoparticle can be obtained. This particle formation condition was valid for both ITO surface and silicon surface. This particle formation of real Ag films on the silicon substrates is shown in Fig. 2. The real 5 nm Ag thin films without any thermal treatment presented in Fig. 2(a) shows that the real Ag films were not so film-like. Because the films in Fig 2(a) is only 5 nm thick, dense islands made of Ag nanocluster seeming like peace of jigsaw puzzle, was formed. After RTA process at 140ºC for 5 minutes, Ag materials were rearranged on the silicon surfaces, making the Ag nanoparticles as seen in Fig 2(b). The inset of Fig. 2(b) shows tilted cross section SEM image of RTA-treated 5 nm Ag films. As seen in the figure, the shape of films was almost sphere-like. However, when the Ag thin films were 6 nm thick, the Ag nanoparticles showed more arbitrary and ellipsoidal shape.

Figure 3 presents the AFM image of Ag nanoparticles on silicon substrates. The deposition condition was perfectly identical except for deposition thickness of Ag thin films. As seen in the AFM images, when the deposition thickness
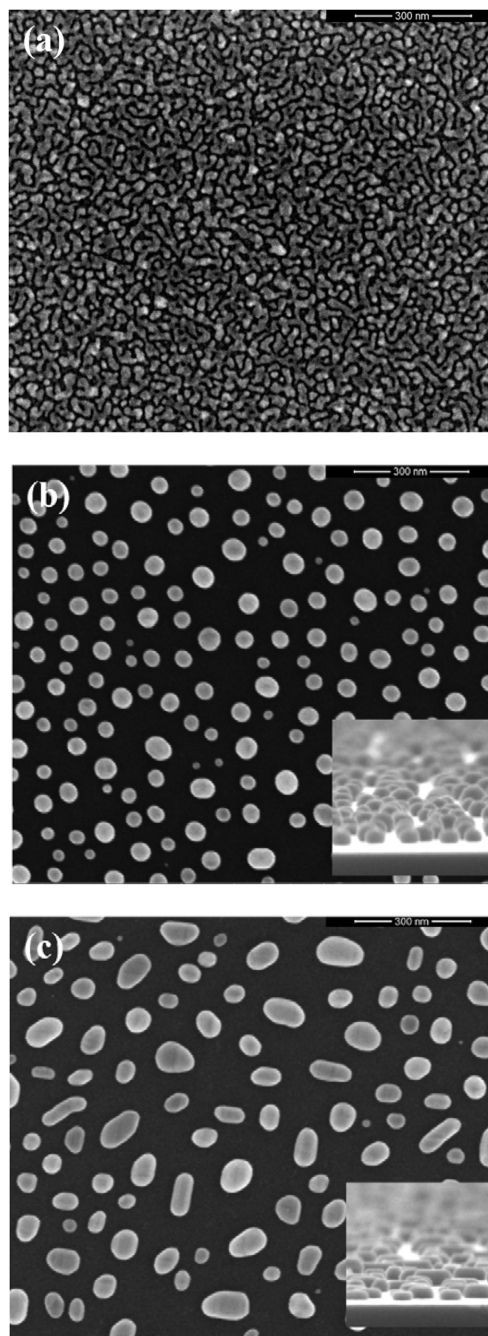
of Ag increased, the particle size of Ag also increased. The analyzed average particle size (diameter) from AFM images was 64.08 nm for Ag 5 nm, 104.8 nm for Ag 6 nm, 159.8 nm for Ag 7 nm, and 156.7 nm for Ag 8 nm. Therefore, the size of particle was saturated after deposition of Ag 7 nm. Also, the peak-to-valley roughness showed very fast increase from Ag 5 nm (9.41 nm) to Ag 7 nm (28 nm), and at deposition of Ag 8 nm, the measured peak-to-valley roughness after RTA treatment was only 31 nm, showing the slow increase. The shape of particles did not
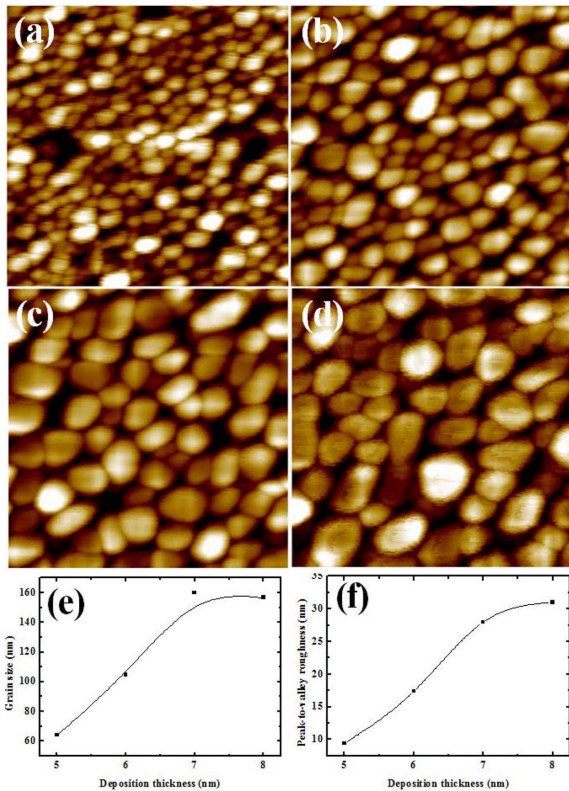
Figure 3. Atomic force microscopy images of Ag nanoparticles of (a) 5 nm, (b) 6 nm, (c) 7 nm, and (d) 8 nm Ag thin film after rapid thermal annealing at 140°C, and (e) the particle size and (f) peak-to-valley roughness calculated using XEI software from AFM images. The resolution of AFM images is 1 μm per figure width and 1 μm per figure length.
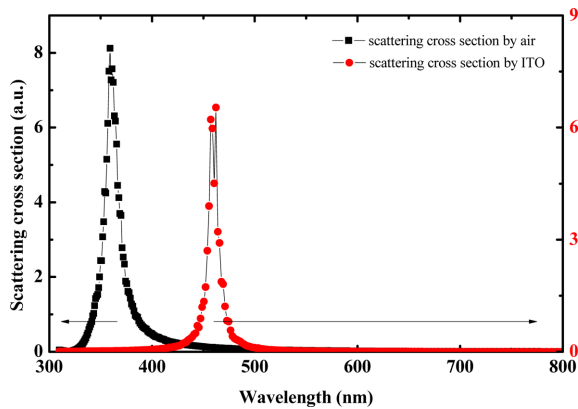
Figure 4. Scattering cross section of silver nanoparticles.

show the big differences in the AFM images during increasing the thickness of Ag due to the possible reasons as follows. The fact that size of particle increased, was obviously identified, but AFM cannot identify what the particles consist of. With SEM, differences of particle kind can be identified as brightness of images. Also, AFM cantilever measures the shape of particle using the oscillation variation of cantilever reacting to atomic force, and the AFM cantilever can only measure the position which the cantilever can touch. Thus, the difference of particle shape between AFM and SEM can occur.
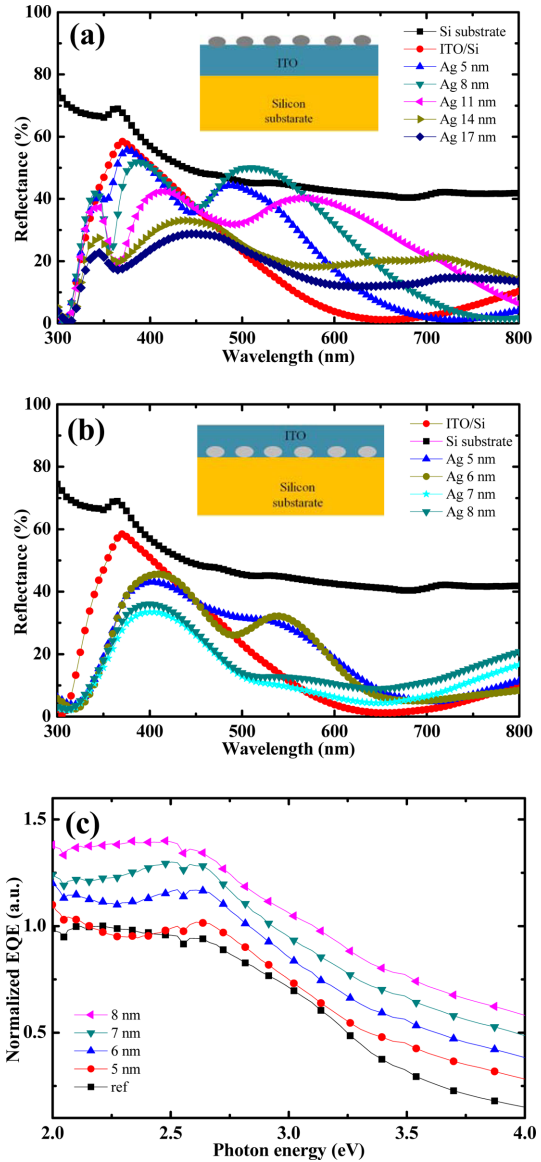
Figure 5. (a) Reflectance of Ag nanoparticle/ITO nm/Si structure, (b) Reflectance of ITO 100 nm/Ag nanoparticle/Si substrate, and (c) normalized external quantum efficiency (EQE) of silicon solar cells (ITO/Ag nanoparticle/Si solar cells).

Figure 4 provides the calculation results of scattering cross section of Ag nanoparticles. The shape of particle was assumed as sphere. The calculation was performed using the formula of Mie scattering under dielectric condition of surrounding environment (air and ITO). The formula for the scattering cross section is as follows [13,14].

$$\sigma_S = \frac{3}{2\pi}\left(\frac{\omega^4}{c}\right)\varepsilon_d^2 \cdot V^2 \frac{(\varepsilon_{1m}-\varepsilon_d)^2+(\varepsilon_{2m})^2}{(\varepsilon_{1m}-2\varepsilon_d)^2+(\varepsilon_{2m})^2}$$

where the ε_d is dielectric constant of surroundings, ε_{1m} is the real part of metal dielectric constant, ε_{2m} is the imaginary part of metal dielectric constant, ω is angular frequency of light, c is the speed of light in vacuum, and V is volume of particle. As seen in Fig. 4, when the Ag

nanoparticle scatter the light in the air, the scattering cross section has strong peak at 358 nm of wavelength, and in the case of ITO, strong peak is found at 460 nm of wavelength. In the practical case, the evidence of scattering can be found in the reflection patterns as seen in Fig. 5(a) and (b).

Figure 5(a) shows the reflection pattern at 30º of incident angle of light for the structure of Ag nanoparticle/ITO/Si substrate. In this case, Ag nanoparticles interact with both air and ITO surface. Therefore, there is reflection suppression found in the particular wavelength. Comparing Fig. 4 with Fig. 5(a), near the 358 nm and 460 nm, there is local minimum point. In the case of structure of ITO/Ag nanoparticle/Si substrates, the local minimum near the resonance peak of Fig. 4 was only found near the 460 nm which is associated with ITO because the Ag nanoparticles are in the ITO films. As seen in Fig. 5(a) and (b), there is red shift of peak with increasing the deposition thickness of Ag. This is considered as shape effect. In the AFM images, the shape variation was not so obvious, but, in the SEM images shown in Fig. 2(b) and (c), when the deposition thickness increased, the shape of Ag nanoparticles varied from sphere to ellipsoid. Figure 5(c) presents normalized external quantum efficiency (EQE) of silicon solar cells with structure of ITO/Ag nanoparticles/Si solar cell. As shown in the figure, there is an enhancement of EQE near 460 nm (2.7 eV) from the Mie theory. This shows that the Ag nanoparticles between ITO and silicon solar cell possibly helps to absorb the selective photons in the plasmonic enhancement range. Also, to find trade-off point of enhancement of EQE, the control of coverage area of silver nanoparticles on the silicon solar cells are necessary.

III. Conclusions

The effect of localized surface plasmon on silicon substrates was studied using silver nanoparticles. The nanoparticles were formed by self-arrangement through the surface energy using rapid thermal annealing (RTA) technique after the thin nano layer of silver was deposited by thermal evaporation. By the theoretical calculation based on Mie scattering and dielectric function of air, indium tin oxide (ITO), and silver, the strong peak of scattering cross section of silver nanoparticles was found at 358 nm for air, and 460 nm for ITO, respectively. Accordingly, the strong suppression of reflectance under the condition of induced light of 30º occurred at the specific wavelength which is almost in accordance with peak of scattering cross section. When EQE was measured using silicon solar cells with silver nanoparticles, there was small enhancement peak near the 460 nm wavelength in which the light was resonated between silver nanoparticles and ITO. It seems that, to find optimized trade-off points to enhance EQE, surface patterning or method from further research is necessary.

Acknowledgements

REFERENCES

[1] R. A. Pala, J. White, E. Barnard, J. Liu, and M. L. Brongersma, Adv. Mater. 21, 3504 (2009).
[2] K. R. Catchpole and A. Polman, Appl. Phys. Lett. 93, 191113 (2008).
[3] K. Nakayama, K. Tanabe, and H. A. Atwater, Appl. Phys. Lett. 93, 121904 (2008).
[4] D.-J. Lee, H.-D. Yim, Y.-G. Kim, Y.-B. Jeong, T. Y. Kim, C. K. Hwangbo, Y. C. Jun, S.-G. Park, S.-G. Lee, and B.-H. O J. Korean Phys. Soc. 63, 2098 (2013).
[5] D.-M. Yeh, C.-F. Huang, C.-Y. Chen, Y.-C. Lu, and C C Yang, Nanotechnology 19, 345201 (2008).
[6] X. Li, W. C. H. Choy, L. Huo, F. Xie, W. E. I. Sha, B. Ding, X. Guo, Y. Li, J. Hou, J. You, and Y. Yang, Adv. Mater. 24, 3046 (2012).
[7] X. Li, W. C. H. Choy, H. Lu, W. E. I. Sha, and A. H. P. Ho, Adv. Funct. Mater. 23, 2728 (2013).
[8] W.-J. Ho, Y.-Y. Lee, C.-H. Hu, and R.-S. Sue, Thin Solid Films doi:10.1016/j.tsf.2016.05.019 (2016).
[9] K. V. Baryshnikova, M. I. Petrov, V. E. Babicheva, and P. A. Belov, Sci. Rep. doi: 10.1038/srep22136 (2016).
[10] D. H. Kim, S. H. Yu, J. Yi, J. H. Kwon, and J. S. Gwag, J. Korean Phys. Soc. 63, 1156 (2013).
[11] T. Minami, Thin Solid Films 516, 1314 (2008).
[12] O. N. Mryasov and A. J. Freeman, Phys. Rev. B 64, 233111 (2001)
[13] S. W. Hsu, K. On, and A. R. Alivisatos, J. Am. Chem. Soc. 134, 3995 (2011).
[14] S.-W. Hsu, W. Bryks, and A. R. Tao, Chem. Mater. 24, 3765 (2012).